Adaptive Locomotion Control of Hexapod Walking Robot for Traversing Rough Terrains with Position Feedback Only

Jan Faigl, Petr Čížek

Authors are with the Czech Technical University, Faculty of Electrical Engineering, Technicka 2, 166 27, Prague, Czech Republic

Abstract

Traversing rough terrains is one of the domains where multi-legged walking robots benefit from their relatively more complex kinematics in comparison to wheeled robots. The complexity of walking robots is usually related not only to mechanical parts but also to servomotors and the necessary electronics to efficiently control such a robotic system. Therefore, large, middle, but even small walking robots capable of traversing rough terrains can be very costly because of all the required equipment. On the other hand, using intelligent servomotors with the position control and feedback, affordable hexapod walking robots are becoming increasingly available. However, additional sensors may still be needed to stabilize the robot motion on rough terrains, e.g., inclinometers or inertial measurement units, force or tactile sensors to detect the ground contact point of the leg foot-tip. In this work, we present a minimalistic approach for adaptive locomotion control using only the servomotors position feedback. Adaptive fine-tuning of the proposed controller is supported by a dynamic model of the robot leg accompanied by the model of the internal servomotor controller. The models enable timely detection of the leg contact point with the ground and reduce developed stress and torques applied to the robot construction and servomotors without any additional sensor feedback. The presented results support that the proposed approach reliably detects the ground contact point, and thus enable traversing rough terrains with small, affordable hexapod walking robot.

Keywords: Multi-Legged Robot, Locomotion Control, Rough Terrains

1. Introduction

Multi-legged robots have a great potential to traverse rough terrains [1] at the cost of relatively more complex robot design and locomotion control in comparison to wheel robots. Although rough terrain traversability capabilities can be enhanced directly by mechanical design of the robot [2], the most of the nowadays multi-legged robots rely on perception or estimation of the contact of the leg foot-tip with the ground, e.g., MAX [3], Weaver [4], HyQ [5], LAURON V [6], AMOS [7], Messor-2 [8], DLR-Crawler [9] to name a few. Individual robots are designed with different intentions but they share many properties allowing them to traverse rough terrains and the main common aspect is the necessary sensory equipment. An open-loop control can be utilized for locomotion control of hexapod walking robots on flat surfaces [10], but additional sensors are required to control attitude over rough terrains [11] (even for biomimetic designs [12]) to achieve self-stabilization by adaptation of feed-forward controllers [13].

In this paper, we address locomotion control over rough terrains using only the position feedback from the servomotors themselves, and thus we propose a minimalistic approach suitable for affordable multi-legged robotic platforms such as the one shown in Fig. 1. Early results on the proposed locomotion control have been reported in [14] and this paper presents an extension of this work with the main contributions as follows.

In the former work, a fixed appropriately selected threshold value for a locomotion control inspired by force threshold-based position (FTP) controller is utilized, and the value has to be experimentally found. The herein proposed approach is based on analysis of the leg motion and the identified dynamic model of the leg motion during the swing-down phase. Accompanied by a model of the controller of the joint servomotor itself, the threshold value is automatically adjusted to be slightly above the expected joint position error provided by the models. The proposed adaptive threshold adjustment has three main advantages over the previous work. First, it is not necessary to perform manual tuning of the threshold value. Second and probably more importantly, there is noticeable static friction and the related dead-zone when the servomotor starts its motion, which causes a high position error at the beginning of the leg swing-down motion. Therefore, the threshold value has to be set sufficiently high to avoid an early stop of the leg which subsequently causes high torque values at the joint when the leg contact with the ground happens (see Fig. 7 with the plot of the herein proposed model-based method of adaptive threshold setting). Moreover, high torque values cause not only harder strikes but also have an impact on the attitude. Besides,

high torque values also mean a high power dissipation and the servomotors can overheat. All these adverse effects of fixed threshold value are avoided by the proposed adaptive model-based method.

In addition to the adaptive threshold settings, the proposed model-based control also enables compensation of limited communication capabilities that can be for example experienced with an affordable robot built from the Dynamixel AX-12A servomotors where all servomotors are connected using daisy chain. Each reading from the servomotor suffers from a transport delay that is especially noticeable when more than a single leg is in the swing-down phase. Therefore, the proposed approach enables to generalize the former method [14] initially developed only for pentapod gait to different gaits, and thus speed up the robot locomotion in rough terrains. The model of the leg and its control by the servomotor controller in the swing-down phase allow predicting the expected position error and thus adjust the threshold appropriately. Also, we further improve the locomotion speed by hardware accelerated readings as it is reported that the utilized Dynamixel AX-12A servomotors suffer from 16 ms period latency when they are used with the serial communication under Windows and Linux-based operating systems [15]. Finally, we report on motion efficiency of the proposed solution with different motion gaits in crawling terrains of various types using the *Cost of Transport* (CoT) [4, 16] as the performance indicator. Regarding the reported results, the proposed method provides more reliable locomotion with lower values of the CoT than the former approach reported in [14].

The remainder of the paper is organized as follows. An overview of the related work is in the following section. The problem statement within the context of the hardware used and existing groundwork is introduced in Section 3. The kinematic model of the robot is presented in Section 4. A summary of the employed body leveling used in [14] is presented in Section 5 to make the paper self-contained. The employed model for the proposed ground detection is presented in Section 6 and its usage in the proposed adaptive locomotion control is proposed in Section 7. Results on the experimental validation are reported in Section 8. Concluding remarks are in Section 9.

2. Related Work

Two complementary types of sensors can be identified for closing the control loop and navigate the robot in rough terrains: the exteroceptive and proprioceptive sensors. Exteroceptive sensors such as cameras or LiDARs [17] provide information for creating a map of the terrain in front of the robot [18] that can be used to control the foot-tips towards the expected foothold positions [11]. In such a map, obstacles can be detected, and a path for the robot can be planned [19] or expected stability of the foothold locations could be estimated [20]. However, a map built online usually represents only a rough approximation of the terrain, and it is not sufficient for precise control of the foot-tips [21], and tactile information may be needed to improve the accuracy [22].

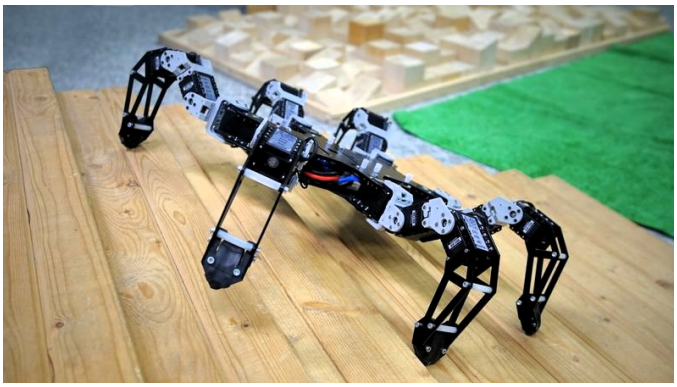

Figure 1: The utilized affordable hexapod walking robot capable of traversing rough terrains by the proposed control method using only the feedback from the servomotors. The robot itself consists only from the trunk, legs formed by 18 Dynamixel AX-12A servomotors, and simple control board of the "Arduino class".

Tactile or force sensors provide proprioceptive signals that can be utilized in reactive controllers [23, 24] or reflex strategies [25, 26] that are sufficient to overcome small obstacles and lightly unstructured terrains. These signals are important for crawling rough terrains to ensure a smooth contact of the foot-tip with the expected foothold, and it is also suggested by the biological studies reporting that force feedback is used for stepping by legged animals [27].

Foothold adaptation based on an online force estimation using torque sensors attached to all robot joints [28] noticeably increase the cost of the robot. A similar setup has been recently proposed by [29] to use the strain gauge type of force sensors for foot-tip force measurements. The authors of [30] consider a 6-DOF force-torque sensor attached to each foot as the tactile sensor. However, the utilized ATI Mini45 F/T sensors significantly increase the cost and complexity of the robot. Force sensitive resistors are utilized by [31] to design a tactile sensing for the Messor robot [32] and this type of sensors has been also used for force-based stability margin [33]. In [34], the authors use a simple pressure sensor connected to a rubber ball that forms a leg foot tip; however, it requires a separate connection per each leg in addition to control of the utilized Dynamixel AX-18A servomotors.

The proprioceptive control of the hexapod Weaver robot [4, 35] uses motor torques estimated from the linear model of the servomotor current. Thus, instead of force-torque sensors, the motor current provided by the utilized Dynamixel MX-64 and Dynamixel MX-106 servomotors is used in the impedance control to adjust the desired foot trajectory; however, foot-strike events are not explicitly detected. The robot motion is achieved by position control of individual joints computed from the foot trajectory using inverse kinematics [4].

The impedance control of the foot trajectory adjust-

ments combined with the position control of individual joints requires a fast control loop with the timely delivered information about the force (torque) and position of the individual joints. The servomotors Dynamixel MX-64 and MX-106 provide such information as they are capable of fast communication; however, they are more expensive than the Dynamixel AX-12 or AX-18 which do not directly provide information about the motor current, and thus the joint torque. In [36], the authors control snake and hexapod walking robots using the measured actuator force that are translated to the desired position command which is then tracked by a low-level position-based controller under the proposed kinematic coupling constraints.

A hexapod walking robot called HexaBull is designed in [37] using a single Dynamixel RX-28 servomotor per each leg that is accompanied by three Dynamixel AX-18A servomotors. However, due to the communication limits of Dynamixel AX-18A, the authors propose a force threshold-based position (FTP) controller for crawling rough terrains [38]. The HexaBull follows existing designs of hexapod walking robots and uses three active servomotors (joints) per each leg. Besides, a passive actuator is used to measure the ground reaction force and substitute direct force sensors. Thus, the HexaBull robot has 18 active actuators, but 24 actuators in the total. The FTP controller [38] operates independently on each leg without interactions with other legs, and thus the achieved leg autonomy is similar to the feed-forward position controller. Although the HexaBull robot does not utilize any additional sensors, it is capable of crawling rough terrains using only the local leg feedback from the additional compliant actuator and without directly sensing the body state [38]. A similar idea of estimating the force at the foot-tip using the torques at the joints is discussed by [39]. However, the torque is estimated from the current of the servomotors measured by an additional Hall effect based sensor.

In this paper, we follow the idea of the FTP controller [37, 38], but we propose an even more minimalistic configuration of the hexapod walking robot with only three actuators per each leg using Dynamixel AX-12A servomotors. Instead of additional compliant servomotor used in the HexaBull robot, we exploit relation of the position error of the built-in position controller of the servomotors to estimate the ground reaction force that can be utilized in the proposed FTP-like controller which uses position information only.[1] The developed solution enables crawling rough terrains with a hexapod walking robot that consists only of 18 servomotors and a simple control board. The main difference of the proposed method to the previous approaches [38, 39] is that our method does not need additional actuators or sensory equipment; hence, it does not increase the cost of the robot nor the complexity of its hardware parts. Besides, the used feedback from the servomotors can be utilized in terrain classification [40] and with additional adjustments [41] for the developed adaptive locomotion control, it can provide fully autonomous navigation of the robot in the road following scenario without any additional sensors [42].

[1] Strictly speaking, the proposed approach is not an FTP controller as it does not directly use a force threshold, but it uses a similar principle to stop the leg motion once the position error is above a particular threshold.

3. Problem Statement and Background

The problem addressed in this paper is to detect the contact point of the leg with the ground, using only the utilized servomotors without any additional sensory feedback. In particular, the used hexapod walking robot consists of 18 Dynamixel AX-12A servomotors, see Fig. 1. The robot does not utilize any additional sensors, and it is constructed purely from the off-the-shelf components, and thus it represents an affordable robotic platform. The platform has six legs, each with three joints directly formed from the Dynamixel actuators, and the particular parts of the leg are depicted in Fig. 2a.

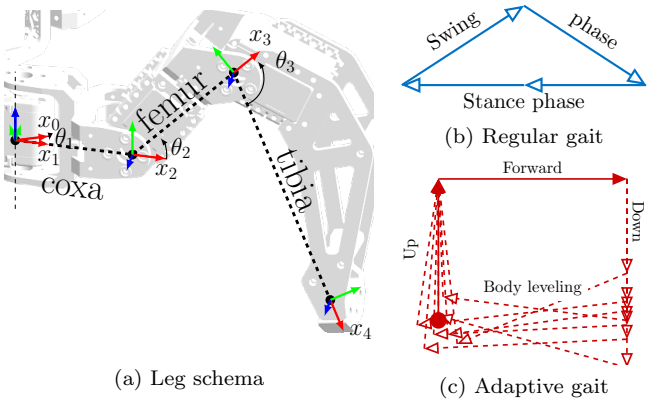

(a) Leg schema (b) Regular gait (c) Adaptive gait

Figure 2: Each leg consisting of three parts (links) denoted coxa, femur, and tibia that are connected by three joints (θ_1, θ_2, and θ_3) indexed according to the next respective link. The joint θ_1 is fixed to the body with the vertical rotation axis, and the two other joints are oriented with respect to the horizontal axis. During the motion, the leg trajectories for a regular gait on a flat terrain form a triangle according to the swing and stance phases, but for the utilized adaptive motion gait with a ground detection, an additional phase for body leveling is applied to adjust the robot posture.

The motion of the robot is realized using a motion gait [43] that prescribes how the particular legs alter in swing and support (stance) phases. Such gaits include *pentapod* gait with only one leg swinging at a time, which is the most stable but also slowest gait in rough terrains [44], *tetrapod* (or amble) gait where four legs are in the supporting phase, and two legs move simultaneously, and the *tripod* (with altering three legs in support and swing phases), which is the fastest stable gait. For all these gaits, the leg motion can be controlled by the position controller. The leg foot-tip follows a prescribed trajectory using position control, and on a flat surface, the trajectory might look like in Fig. 2b.

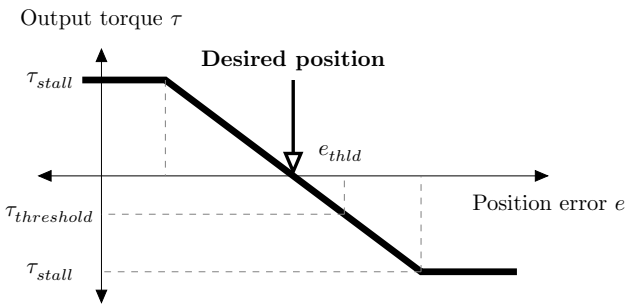

Figure 3: The relation of the torque τ and the position error e for a steady state of the utilized Dynamixel AX-12A. The value of τ is limited by a stall torque value τ_{stall}.

For rough terrains, the motion has to adapt to the terrain, and the motion of the individual leg can be adapted by the controller using the provided feedback from the servomotors [14]. The locomotion control is split to movement of individual legs followed by the body movement (further denoted as body leveling). The separation of the leg and body movements allows us to consider a simplified model of the leg dynamics consisting of only two servomotors because only two joints are active during the swing down phase. The explicit forward motion is added to speed up the robot forward velocity because the position error based ground detection is performed in the swing-down phase and it requires slower motion to avoid high torques. Thus, the leg trajectories can look like in Fig. 2c.

The ground detection relies on measuring the ground reaction force as a result of the leg contact with the ground. The source of the force is the torque at the leg joints. For the Dynamixel AX-12A, the torque is considered to be proportional to the position error according to Fig. 3. Even though the servomotor provides the joint angle and the estimated torque values, the position values are more reliable [14]. However, the relation in Fig. 3 holds only for a steady state, and the position error value is not an instant measurement of the ground reaction force/torque. Therefore it is necessary to limit the expected position error during the leg swing-down motion to make the relation between the position error and the torque usable. Otherwise, the position error would be high at the beginning of the swing-down phase while the leg can still be above the ground. Therefore, the leg movement in the swing-down phase is interpolated by small steps to achieve sufficiently small differences between the desired and the current position of the joint angle. The interpolation is also necessary to detect the ground and stop the leg motion in an instant the leg reaches the ground to avoid the increase of the ground-reaction force. If the leg is not stopped, the whole robot may elevate, and some other legs may lose the ground support, which could further lead to slippage. Moreover, the used Dynamixel AX-12A servomotors support a stable motion for the loads with 1/5 or less of the stall torque and increased torque result in servomotor overheating or its damage [14].

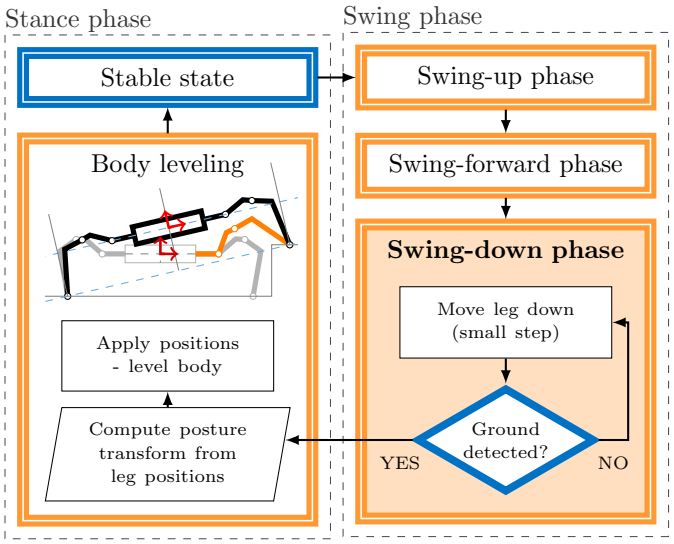

Figure 4: Schema of the locomotion control with the ground detection in the leg swing-down phase, where the trajectory is interpolated for estimating the torque at the servomotor joint from its position data. If more legs are active in the swing-down phase, e.g., for the tripod gait, all legs are controlled simultaneously, and the body leveling is performed after all moving legs finished the swing-down phase.

The schema of the considered locomotion control is depicted in Fig. 4 and it has been firstly introduced in [14]. The gait cycle consists of the swing phase and stance phase where the body leveling is performed. The swing phase starts with the swing-up when the active legs leave their footholds, then continues with the swing-forward. The leg motion is terminated in the swing-down phase when the legs start approaching the ground. Once the ground is detected, the leg motion is stopped by setting the desired position of the individual joints to maintain the appropriate ground reaction force. The position and rotation of the body are then adjusted to fit with new positions of the legs and align the body with the terrain.

In addition, the real position error is not an instant measurement, and the limited communication of the Dynamixel AX-12A makes the detection even more challenging. The servomotors communicate via a half-duplex serial line connected to a serial bus. Moreover, the position data can be read from a single servomotor only every 16 ms (in a standard setup as reported in [15]), which is relatively very high considering the robot has 18 actuators. Fortunately, the joint θ_2 (femur link) reflects the most of the overall ground reaction force, albeit the momentum acts on the θ_2 and θ_3 joints (see Fig. 2a) as well. Regarding the preliminary results for a hand-tuned single fixed value of the position error threshold e_{thld} reported in [14], position data solely from θ_2 are considered sufficient.

Preliminary results on the locomotion control are reported in our early work [14] but its main drawback is in the hand-tuned e_{thld} specifically found for the used robot with only a single leg movement in the pentapod gait. An appropriate value of e_{thld} depends on the weight of the

legs, the positions of the legs when reaching the ground, and also on the velocity of the movement, which all affect the acting momentum before the leg reaches the ground. Besides, position readouts can be delayed, e.g., as for the Dynamixel AX-12A servomotors, which makes setting appropriate values of e_{thld} difficult, e.g., for tripod gait.

Therefore, the herein addressed problem is to not rely on the torque/error relation according to Fig. 3 but rather estimate the position error that is computed by a dynamic model of the leg motion during the swing-down phase combined with the model of the servomotor internal position controller. We aim to design an approach for adaptive settings of the appropriate values of e_{thld} during the robot motion and thus avoid laborious hand-tuning and further support generalization of the locomotion control for different motion gaits and different robots.

4. Kinematic model of the robot

In the locomotion control based on motion gaits, repetitive trajectories for individual legs describe the desired position of the leg foot-tip and the joint angles needed for the actuators have to be computed from the trajectories using the inverse kinematics. Besides, forward kinematics is needed in the body leveling to adjust the robot posture. Therefore both the forward and inverse kinematics are the needed preliminaries.

4.1. Forward Kinematics

The kinematic model of the used 18-DOF robot can be based on Denavit–Hartenberg (DH) convention. Five Cartesian coordinate systems cover the path from the body to the foot with four of them relative to the leg as it is depicted in Fig. 2a. The transformation matrix between two adjacent leg coordinate systems can be expressed in the DH convention as

$$\mathbf{M}_i^{i-1} = \begin{bmatrix} c_{\psi_i} & -s_{\psi_i}\, c_{\alpha_i} & s_{\psi_i}\, s_{\alpha_i} & a_i\, c_{\psi_i} \\ s_{\psi_i} & c_{\psi_i}\, c_{\alpha_i} & -c_{\psi_i}\, s_{\alpha_i} & a_i\, s_{\psi_i} \\ 0 & s_{\alpha_i} & c_{\alpha_i} & d_i \\ 0 & 0 & 0 & 1 \end{bmatrix}, \quad (1)$$
$$\psi_i = \theta_i + \theta_i^{off},$$

where c_{ψ_i} and s_{ψ_i} denote $\cos(\psi_i)$ and $\sin(\psi_i)$, respectively, and $\alpha, a, \theta, \theta^{off}, d$ are the DH parameters with the particular values listed in Table 1.

Table 1: Values of the Denavit–Hartenberg Parameters

Link	i	α_i [rad]	a_i [mm]	d_i [mm]	θ_i^{off} [rad]	θ_i [rad]
Coxa	1	$\pi/2$	52	0	0	θ_1^l
Femur	2	0	66	0	-0.22	θ_2^l
Tibia	3	0	138	0	-0.81	θ_3^l

Let ${}^0\mathbf{p}$ be the foot-tip position of the leg in the coordinate system relative to the body and ${}^4\mathbf{p}$ be the foot-tip position in the foot-tip coordinate system. Then the mapping between the body coordinate system and the foot-tip coordinate system is given by the following kinematic chain

$$\begin{bmatrix} {}^0\mathbf{p} \\ 1 \end{bmatrix} = \mathbf{T}^l\, \mathbf{M}_1^0\, \mathbf{M}_2^1\, \mathbf{M}_3^2 \begin{bmatrix} {}^4\mathbf{p} \\ 1 \end{bmatrix}, \quad (2)$$

where $\mathbf{T}^l$ is the transformation matrix between the body coordinate frame and the coxa coordinate frame of the l-th leg given as rigid body transformation

$$\mathbf{T}^l = \begin{bmatrix} \cos_{\beta^l} & -\sin_{\beta^l} & 0 & p_x^l \\ \sin_{\beta^l} & \cos_{\beta^l} & 0 & p_y^l \\ 0 & 0 & 1 & 0 \\ 0 & 0 & 0 & 1 \end{bmatrix}, \quad (3)$$

where β^l, p_x^l, and p_y^l are the body parameters of the l-th link listed in Table 2.

Table 2: Body parameters

l	1	2	3	4	5	6
β^l	$\pi/4$	$7\pi/4$	$3\pi/4$	$5\pi/4$	$\pi/2$	$3\pi/2$
p_x^l	120.6	120.6	-120.6	-120.6	0	0
p_y^l	60.5	-60.5	60.5	-60.5	100.5	100.5

The values of β^l are in rad, the values of p_x^l and p_y^l are in mm.

4.2. Inverse Kinematics

The selected configuration of joints greatly simplifies the inverse kinematics task. Given the foot-tip coordinates ${}^0\mathbf{p} = [{}^0p_1, {}^0p_2, {}^0p_3]$ in the global coordinates, we can obtain the coxa joint angle θ_1^l of the l-th leg as

$$\theta_1^l = \arctan\left(\frac{{}^0p_1 - p_x^l}{{}^0p_2 - p_y^l}\right) - \beta^k. \quad (4)$$

The coordinates ${}^0\mathbf{p} = (p_1, p_2, p_3)$ expressed relatively to the femur coordinate frame yield the following equation

$${}^2\mathbf{p} = \left[\sqrt{{}^0p_1^2 + {}^0p_2^2} - a_1, {}^0p_3, 0\right]^T. \quad (5)$$

The respective femur θ_2^l and tibia θ_3^l angles are then given according to the cosine law and the angle above the horizon

$$\theta_2^l = \arccos\left(\frac{a_2^2 - a_3^2 + \left\|{}^2\mathbf{p}\right\|^2}{2a_2\left\|{}^2\mathbf{p}\right\|}\right) - \arctan\left(\frac{{}^2p_2}{{}^2p_1}\right) - \theta_2^{Off}, \quad (6)$$

$$\theta_3^l = \pi - \arccos\left(\frac{a_2^2 + a_3^2 - \left\|{}^2\mathbf{p}\right\|^2}{2a_2a_3}\right) - \theta_3^{Off}. \quad (7)$$

5. Body Leveling and Robot Movement

In the adaptive motion gait, see Fig. 4, the body motion is separated from the leg motion, and the body has to counteract changed legs footholds by shifting and rotating into a more suitable posture. The robot may walk over rough terrains, and it is completely without any perception about the terrain ahead, and thus there is no option to choose any preferable body posture to prepare for the forthcoming terrain. Therefore, the proposed body leveling is a movement into an *equilibrium body position* that offers balanced possibilities of the movement in all directions. The idea of the body leveling is visualized in Fig. 5. Various approaches can be utilized to compute the desired joint angles, e.g., using Singular Value Decomposition [45], but also by a straightforward computation based on a forward movement of the body used in this work, which can be performed in the following steps.

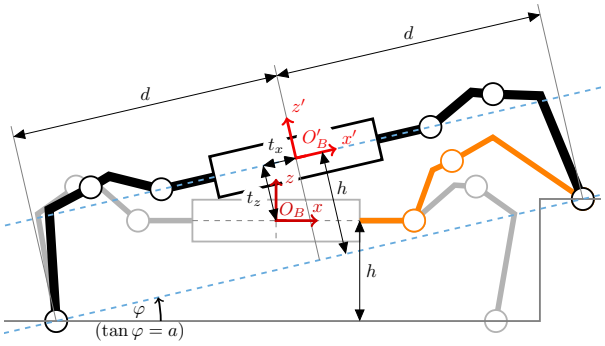

Figure 5: An overview of the body leveling strategy to align the robot body with the terrain. Once the active leg (in gray) reaches a new foothold position (in orange), the posture of the body is adjusted by a new configuration of the legs (in black) to maintain the same distances of h and d.

First, the plane ρ minimizing the squared distance to the leg foot-tip positions is determined as $z = a_\rho x + b_\rho y + c_\rho$. Then, the body posture transformation between the original body coordinate frame ${}^0\boldsymbol{p}_B$ and the new coordinate frame ${}^0\boldsymbol{p}'_B$ is found to improve stability and leg working space margins

$$\begin{bmatrix} {}^0\boldsymbol{p}'_B \\ 1 \end{bmatrix} = \begin{bmatrix} \boldsymbol{R} & \boldsymbol{Rt} \\ \boldsymbol{0} & 1 \end{bmatrix} \begin{bmatrix} {}^0\boldsymbol{p}_B \\ 1 \end{bmatrix}, \tag{8}$$

where $\boldsymbol{R}$ and $\boldsymbol{t}$ are the body rotation matrix and translation vector, respectively. The matrix $\boldsymbol{R}$ can be expressed as

$$\boldsymbol{R} = \begin{bmatrix} \boldsymbol{b}_x & \boldsymbol{b}_y & \boldsymbol{b}_z \\ & & \end{bmatrix} \begin{bmatrix} \|\boldsymbol{b}_x\| & 0 & 0 \\ 0 & \|\boldsymbol{b}_y\| & 0 \\ 0 & 0 & \|\boldsymbol{b}_z\| \end{bmatrix}^{-1} \tag{9}$$

which is formed from the basis vectors of the orthonormal coordinate frame bounded with the regression plane ρ such that $\boldsymbol{b}_x = (1, 0, a_\rho)^T$ is the vector preserving the forward walking direction, $\boldsymbol{b}_z = (-a_\rho, -b_\rho, 1)^T$ is orthogonal to the ρ plane, and $\boldsymbol{b}_y = (-a_\rho b_\rho, a_\rho^2 + 1, b_\rho)^T$ is selected to form orthogonal basis together with $\boldsymbol{b}_x$ and $\boldsymbol{b}_z$. The translational vector $\boldsymbol{t}$ is given as

$$\boldsymbol{t} = \begin{bmatrix} \dfrac{\sum_{l=1}^{6} x_l + a_\rho \sum_{l=1}^{6} z_l}{6\,\|\boldsymbol{b}_x\|} \\ \dfrac{-a_\rho b_\rho \sum_{l=1}^{6} x_l + (a_\rho^2 + 1) \sum_{l=1}^{6} y_l + b_\rho \sum_{l=1}^{6} z_l}{6\,\|\boldsymbol{b}_y\|} \\ \dfrac{c_\rho}{\|\boldsymbol{b}_z\|} \end{bmatrix}, \tag{10}$$

where (x_l, y_l, z_l) are the l-th leg foot-tip coordinates in the global reference frame.

Finally, the body movement is achieved by applying the forward transformation of (8) to all the leg coordinates and motion execution to get the legs to their new positions. Since the legs are always moving forward—through the distance between the new and old foot positions is variable—and the body position is computed as an average of the new foot positions, the body is therefore always following the legs which make the whole robot move in the desired direction.

6. Model of the Leg Swing-Down Phase

The proposed adaptive locomotion control is based on the evaluation of the joint position error of the servomotor during the leg swing-down phase, when only two joints are active. The fundamental idea is to stop the leg motion when the position error is high, which is assumed to be caused by the ground reaction force that does not allow the leg to continue its motion, and thus the joint position error is increasing. Contrary to the previous approach [14] that uses a fixed threshold value of the position error, we propose an adaptive mechanism to automatically adjust the appropriate threshold value based on the model of the leg motion.

In particular, the dynamics of the leg is modeled together with the simulation of the internal servomotor controller to provide a prediction of the expected position error. The model assumes free leg motion in the swing-down phase without the contact of the leg with the ground, and therefore, the ground reaction force applied to the leg, when it touches the ground, increases the position error that is then utilized to detect the ground contact. Thus, the value of the position error above the particular threshold can trigger the locomotion controller to stop the leg motion. Then, once all legs in the swing-down phase are stopped, the body leveling can be applied to reach the stable state, and the locomotion control may continue with the swing phase for the alternating legs as shown in Fig. 4.

The required model consists of the dynamic model that can be derived using the Euler-Lagrange method [46] where only two joint angles corresponding to actuators attached to the femur and tibia are employed, which are the only active servomotors in the leg swing-down phase. Besides, we need to consider the actuator dynamics to model

frictions and the initial dead zone of the servomotor when the servomotor moves from the steady state. Finally, we also need to identify and model the internal P-type controller of the servomotor to predict the expected position error for the case of zero ground reaction force.

The model of the leg motion is based on the model of the chain of rigid bodies for a two-link system moving in a plane because only the femur and tibia links are moving in the swing-down phase. The model can be derived using Euler-Lagrange method, e.g., see Section 7.3.2 of [46], and for the vector $\boldsymbol{q} = (\theta_2, \theta_3)$ of the generalized coordinates, the model can be expressed as by the equation

$$\boldsymbol{D}(\boldsymbol{q})\ddot{\boldsymbol{q}} + \boldsymbol{C}(\boldsymbol{q}, \dot{\boldsymbol{q}})\dot{\boldsymbol{q}} + \boldsymbol{G}(\boldsymbol{q}) = \boldsymbol{\tau}, \tag{11}$$

where $\boldsymbol{D}(\boldsymbol{q})$ is 2×2 symmetric, positive definite inertia matrix of the two joints, $\boldsymbol{C}(\boldsymbol{q}, \dot{\boldsymbol{q}})$ is a tensor that represents the centrifugal and Coriolis effects induced on the joints, $\boldsymbol{G}(\boldsymbol{q})$ is the vector of moments generated at the joints by the gravitational acceleration, and $\boldsymbol{\tau}$ is the vector of actuation torques at the respective joints.

The model described by (11) is sufficient for controlling robotic platforms that provide the torque readings. However, the utilized Dynamixel AX-12A actuators do not provide the torque readings, and therefore, it is needed to model the servomotor with its controller to determine the expected position of the joint actuators influenced by the leg dynamics.

In the studied case, the real actuator is composed of the motor and reduction gear which dynamics can be expressed as

$$J\ddot{q}^M + B\dot{q}^M + F(\dot{q}^M) + R\tau = K\,V, \tag{12}$$

where q^M is the rotor position angle before reduction, J is the rotor inertia, B is the rotor damping, F is a sum of static, dynamic, and viscous friction that depends on the current rotor speed, R is the gearbox ratio, τ is the servomotor torque, K is the back electromotive force, and V is the motor voltage. The appropriate value of the parameters J, B, F, R, and K have to be experimentally identified using the real servomotor or the values specified in the manufacturer data sheet can be utilized. The particular values of the parameters are listed in Table 3, where τ^c is the Coulomb friction coefficient that is the only friction considered.

Table 3: Model Parameters of Dynamixel AX-12A

Parameter	Value	Unit
J	$1.03 \cdot 10^{-7}$	kg·m^2
B	$3.12 \cdot 10^{-6}$	N·m·s
R	$254:1$	-
K	$3.91 \cdot 10^{-3}$	N·m·A^{-1}
τ^c	$2.37 \cdot 10^{-4}$	N·m

The P-type position controller influences the voltage V that can be modeled as

$$V = k_P \cdot err, \tag{13}$$

where k_P is the controller gain, and err is the difference between the set and current position, which is internally updated in the servomotor with 1 kHz frequency. Therefore, the same frequency is utilized for the simulation of the servomotor control.

The desired complete dynamics of the leg in the joint variables can be derived by substituting (12) into (11) as

$$\begin{aligned}(\boldsymbol{J} + \boldsymbol{R}^2\boldsymbol{D}(\boldsymbol{q}))\ddot{\boldsymbol{q}} + (\boldsymbol{B} + \boldsymbol{R}^2\boldsymbol{C}(\boldsymbol{q}, \dot{\boldsymbol{q}}))\dot{\boldsymbol{q}} + \boldsymbol{R}\boldsymbol{F}(\dot{\boldsymbol{q}}) + \\ \boldsymbol{R}^2\boldsymbol{G}(\boldsymbol{q}) = \boldsymbol{R}\boldsymbol{K}\boldsymbol{V},\end{aligned} \tag{14}$$

where the scalars of (12) become vectors and corresponding matrices because of two joint variables θ_2 and θ_3 considered as the generalized coordinates $\boldsymbol{q}$. Note, the model is valid only for the leg swing down phase with movement of the femur and tibia joints, which in fact is enabled by the separated leg movement and body leveling.

In the proposed control schema, the dynamic model is employed in determining the estimated value of the current femur joint position θ_{est} by simulating the leg motion according to the requested positions of the moving joints. Besides, the servomotor positions are computed with the 1 ms granularity, i.e., the model can be queried for the position error at any given instant which allows overcoming possibly delayed readouts.

7. Adaptive Locomotion Control

The proposed adaptive locomotion control is based on the ground detection method that solely utilizes the position controller that stops the motion when the joint position error is above the error threshold e_{thld}. The proposed controller fits the overall locomotion control schema depicted in Fig. 4 and it also uses interpolation of the joint trajectory during the leg swing-down phase. However, we employ a model of the leg dynamics during the swing-down phase including the model of the internal servomotor controller to predict the expected position error. Hence the threshold value e_{thld} is updated at the every k-th step of the control loop that works with the period t_{con}, and thus the threshold is considered as $e_{thld}(k)$.

The ground detection is schematically depicted in Fig. 6, which is for simplicity visualized only for a single servomotor, i.e., a position control of the femur actuator, of a single leg. The trajectory interpolation is used similarly to [14] because the position error is not an instant measurement and it is desired to avoid high torques. The control cycle is performed with the period t_{con} and it starts with the initial joint position θ_{init} to reach the desired position θ_{des} in the requested period t_{des}. All these values come from the particular motion gait, and they define the expected behavior

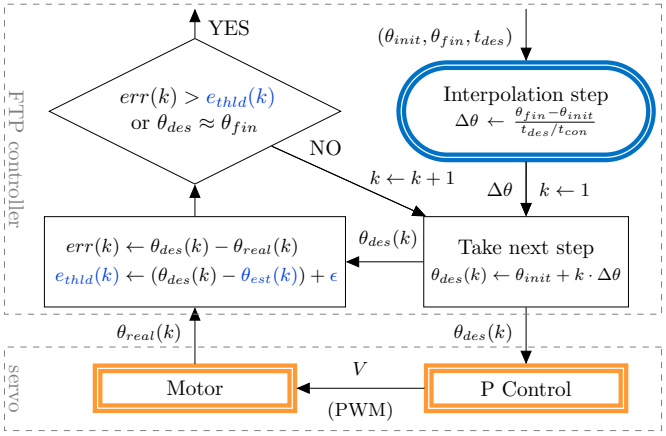

Figure 6: The control cycle of the proposed position threshold based controller with trajectory interpolation during the leg swing-down phase. For every step k of the control cycle, the desired joint position $\theta_{des}(k)$ is updated by a small distance $\Delta\theta$ to be traveled in the period t_{con}. $\theta_{des}(k)$ is then sent to the P-type controller of the servomotor that produces the corresponding value of the Pulse Width Modulation (PWM) to control the motor. The read position of the joint $\theta_{real}(k)$ is used to compute the error $err(k)$. The particular threshold value $e_{thld}(k)$ is computed from the estimated position $e_{est}(k)$ using the developed dynamic model. If $err(k)$ is above e_{thld}, the ground has been reached; otherwise, the procedure is repeated until the ground is detected or the final position θ_{fin} is reached.

in the leg swing-down phase. The increment of the joint position as the interpolation step $\Delta\theta$ can be computed as

$$\Delta\theta = \frac{\theta_{fin} - \theta_{init}}{t_{des}/t_{con}}. \tag{15}$$

Then, the desired joint position $\theta_{des}(k)$ for the k-th control step is updated and send to the servomotor as a new setpoint. The real measured joint position $\theta_{real}(k)$ and $\theta_{des}(k)$ are used to compute the position error. However, the measured position value does not necessarily be the current real joint position because of the communication delay. Thus, we employ the model of the leg swing-down phase to estimate the joint position as $\theta_{est}(k)$ that is compared with the measured position error. Since the comparison depends on the direction of the motion and orientation of the servomotor, i.e., how it is attached to the leg link, the position errors are considered for the comparison and thresholding

$$err(k) = \theta_{des}(k) - \theta_{real}(k), \tag{16}$$
$$e_{thld}(k) = \theta_{des}(k) - \theta_{est}(k) + \epsilon, \tag{17}$$

where the value of ϵ is experimentally found adjustment parameter to compensate the joint angle value discretization and mechanical inaccuracies of the particular leg. The used value is $\epsilon = 3$ ticks, which is less than 1°. Finally, the leg control is stopped when the ground is detected, or the joint reaches the requested position θ_{fin}.

The values of θ_{fin} are set such that, the leg foot-tip is requested to go under the ground in crawling on flat terrain to develop the ground-reaction force, and thus detect the ground and stop the leg motion. Notice the leg motion can be effectively stopped by setting $\Delta\theta = 0$ for all the leg servomotors. The fundamental idea of the proposed ground detection is that the model of the leg swing-down phase does not include the ground reaction force, and therefore, θ_{real} should be close to θ_{est} during the leg motion unless the servomotor is influenced by the ground reaction force, and thus the leg touches the ground.

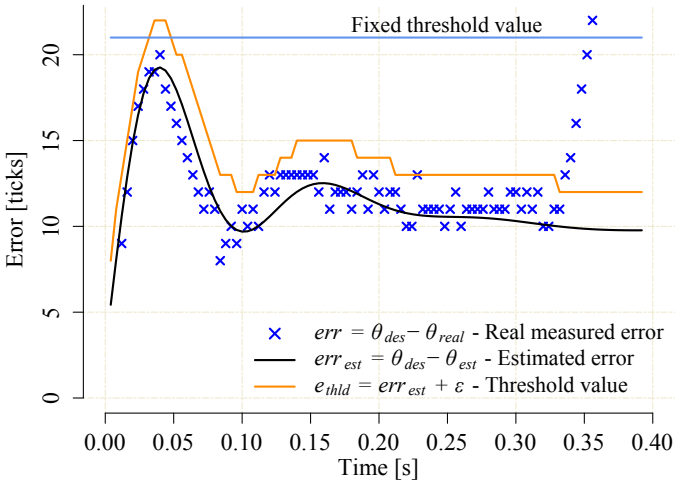

Figure 7: Measured and estimated position errors of the femur actuator. The threshold value e_{thld} is derived from the estimated error increased about three ticks $\epsilon = 3$ to consider imperfections in the model identifications. The measured positions θ_{real} are read out at every control cycle which works with the period $t_{con} = 3$ ms because of communication limits.

The model is crucial to automatically set an appropriate threshold value based on the whole kinematic chain of the leg, which is not captured by the steady state relation of the position error and the motor torque shown in Fig. 3. Therefore we propose to detect the ground, not by the direct usage of the relation shown in Fig. 3, but rather by monitoring the measured real position of the joint θ_{real} and its comparison with the estimated joint position θ_{est} provided by the model. An example of the estimated position error err_{est} and the real measured error err is depicted in Fig. 7. The peak around 0.05 s is because the leg motion is initiated from a steady state and the leg motion develops a joint torque that is caused by the initiated motion of the whole kinematic chain of the leg, which is the most critical part for the employed model.

For the fixed threshold value, it is necessary to select the threshold high enough to avoid a premature stop of the motion as we did in [14]. However, a higher threshold value increases the error and thus the joint torques. Therefore unnecessarily high threshold values cause high torques when the leg touches the ground, and the servomotors may consequently overheat, which can be observed for the previous approach [14] deployed in a long mission. Note the joint positions and position errors are reported in ticks to express the utilized values precisely.

Besides the prediction of the peak in the position error

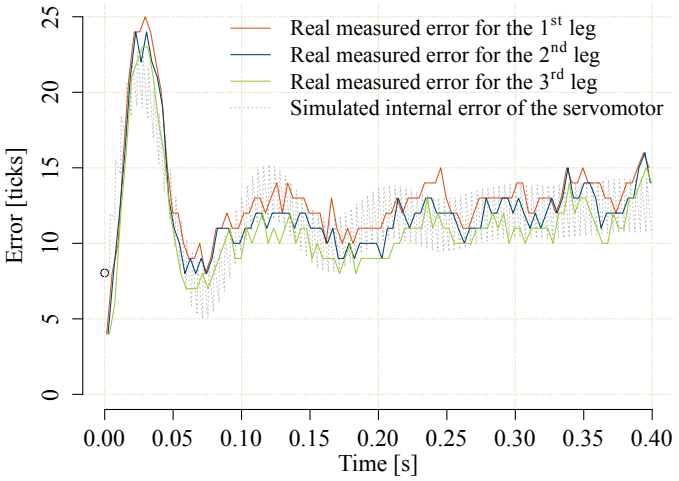

Figure 8: Example of the measured and estimated errors during simultaneous motion of three legs in the tripod gait. The control cycle period t_{con} is $t_{con} = 3T_{com}$. Because of $T_{com} = 1$ ms, the readout of the real measured position error is delayed for the third leg, and the joint position already travels towards the new setpoint, and thus the position error is lower than for the first readout joint position. The servomotors of all active legs are commanded simultaneously, and therefore, the evolution of the estimated error corresponds to all of them. The values of θ_{est} are computed using the model of the leg motion in the swing-down phase that also includes the model of the servomotor internal P-type position controller running with the control period 1 ms.

at the beginning of the leg swing-down phase, the model is also useful in compensating the delay in reading the current joint position which is not available instantly. In particular, there can be a communication delay $T_{com} = 16$ ms for a single read operation for the utilized Dynamixel AX-12A servomotors with the standard readings over the serial communication interface under Windows or Linux operating systems that is reported in [15]. Even though the delay can be reduced by hardware accelerated communication to 1 ms for a single read operation, the delay may still affect the position error, especially when multiple legs are simultaneously in the swing-down phase, e.g., in the tripod gait. It is because the positions are read out sequentially since all servomotors are connected to the same communication bus with a half-duplex serial protocol, and all the servomotors are commanded simultaneously to keep the motion synchronized. Thus, it may happen that for the last read position, the particular joint already traveled a significant portion of the desired trajectory, and the position error is lower than for the readout position error for the first servomotor. An example of the particular position errors during the swing-down phase of the tripod gait with three simultaneously controlled legs is depicted in Fig. 8. It can be noticed in the figure, that the errors differ depending on the time when the position is read out from the particular servo. In this case, the control cycle period is $t_{con} = 3T_{com}$ because it is delayed by three readouts from the servomotors, i.e., each readout takes $T_{com} = 1$ ms, and therefore, the readout of the real measured position error for the third servo is noticeably delayed and the servo already travels towards its θ_{des}, and thus its error is lower, which also holds for the estimated error.

Algorithm 1: Ground detection using position feedback

Input: $\boldsymbol{\theta}_{init} = \{\boldsymbol{\theta}^1_{init}, \ldots, \boldsymbol{\theta}^L_{init}\}$ – the initial joint angles of femur and tibia servomotors $\boldsymbol{\theta}^l_{init}$ of all active legs, $\boldsymbol{\theta}^l_{init} = \{\theta^l_{2,init}, \theta^l_{3,init}\}$ for $1 \leq l \leq L$, where L is the number of active legs

Input: $\boldsymbol{\theta}_{fin} = \{\boldsymbol{\theta}^1_{fin}, \ldots, \boldsymbol{\theta}^L_{fin}\}$ – the requested final joint angles of the employed servomotors, $\boldsymbol{\theta}^l_{fin} = \{\theta^l_{2,fin}, \theta^l_{3,fin}\}$ for $1 \leq l \leq L$

Input: t_{des} – the desired time of the swing-down motion

Input: T_{com} – the communication delay $T_{com} = 1$ ms

$t_{con} \leftarrow L \cdot T_{com}$ `// set the control period`

for servo $i \in \{2, 3\}$ of each active leg $l \in \{1, \ldots, L\}$ **do**

  $\Delta\theta^l_i \leftarrow$ `CalcStep`$(\theta^l_{i,init}, \theta^l_{i,des}, t_{des}, t_{con})$ `// (15)`

$t \leftarrow 0$ `// reset swing-down phase control time`

while not all legs stopped **do**

  for each $i \in \{2, 3\}$ and $l \in \{1, \ldots, L\}$ **do**

    $\theta^l_{i,des} \leftarrow \theta^l_{i,des} + \Delta\theta^l_i$ `// interpolation step`

  `SetAllServoPositions`$(\boldsymbol{\theta}^1_{des}, \ldots, \boldsymbol{\theta}^L_{des})$

  for each active leg $l \in \{1, \ldots, L\}$ **do**

    $\theta_{real} \leftarrow$ `ReadServoPosition`$(l, 2)$ `// femur`

    $\theta_{est} \leftarrow$ `CalcModel`$(l, \theta^l_{2,des}, \theta^l_{3,des}, t)$

    $err \leftarrow \theta^l_{2,des} - \theta_{real}$ `// femur` $i = 2$

    $e_{thld} \leftarrow \theta^l_{2,des} - \theta_{est} + \epsilon$ `// femur` $i = 2$

    if $err > e_{thld}$ *or* $\theta^l_{2,des} \approx \theta^l_{2,fin}$ **then**

      $\Delta\theta^l_2 = \Delta\theta^l_3 = 0$ `// stop the` l`-th leg`

    $t \leftarrow t + T_{com}$ `// increase` t `because of the communication delay`

Only the femur and tibia actuators are controlled, the position of the coxa actuator is fixed to its last position from the swing-forward phase.

The proposed ground detection in the swing-down phase using the position feedback with simultaneous motion of multiple legs is summarized in Algorithm 1 and implementation of the proposed adaptive locomotion control is available in [47]. Since the femur and tibia servomotors of the active legs in the swing-down phase are controlled, the particular leg is identified by the superscript and the individual servos per each leg are identified by the subscript i according to Table 1. All the computations and procedures are considered to be instant except calling the `ReadServoPosition()` procedure that takes a significant time T_{com} that has to be taken into account during the model calculation in the procedure `CalcModel()`. The initial and desired position together with the time t_{des} are set according to the motion gait when switching from the stance phase to the swing phase. Results on the real per-

formance of the proposed ground detection method are reported in the following section.

8. Experimental Results

The developed adaptive locomotion control with the proposed model-based ground detection has been experimentally verified in practical deployments. Its performance is compared with the former approach [14] despite several other approaches have been proposed in the literature. It is mainly because the proposed approach solely uses the position feedback while other approaches have been proposed for different robots and rely on specific additional sensors. Thus, the main intention of the reported results is to demonstrate the feasibility of the proposed minimalistic solution in traversing rough terrains. Besides, a deployment of other approaches requires force or torque measurements that are not available for the utilized affordable hexapod walking robot without any additional sensors. Therefore, we designed four experimental scenarios to show the main properties of the proposed adaptive locomotion control. In the first scenario, we experimentally verify the behavior of the developed dynamic model employed in the estimation of the position error for increasing the speed of the leg motion. The second scenario is focused on analyzing the locomotion stability for three motion gaits employed in traversing rough terrains. In the third scenario, we consider the Cost of Transport (CoT) measure [48, 4] to evaluate the performance of the proposed locomotion control in comparison with the former approach [14] for different leg motion speeds and three motion gaits in traversing different terrains. Finally, we evaluate the impact of the adaptive thresholding to the reliability of the locomotion, and we verify lower torque values in comparison to the former approach [14] by measuring temperature evolution while traversing rough terrain.

8.1. Position Error Estimation using the Dynamic Model

The leg movement during the swing-down phase involves motion of the femur and tibia servomotors which moves according to the proposed control scheme described in Section 7. The motion of each servomotor is subject to (15) which can be influenced by the values of t_{con} and t_{des}. The value of the period t_{con} is limited by the communication constraints and by the number of simultaneously operating servomotors, and thus its minimal value is defined by the hardware used. On the other hand, the period t_{des} is a user-defined value, and it influences the speed of the servomotor which has a direct impact to the developed joint torque at the moment of the leg contact with the ground. Besides, it also influences the robot movement, and shorter values mean faster leg motion and thus faster robot movement.

The performance of the model has been studied in an experimental setup with different leg motion speeds given by t_{des}. In particular, the influence of t_{des} has been experimentally studied for $t_{des} \in \{0.5, 1.0, 2.0\}$ seconds for the fastest control period $t_{con} = 3$ ms (tripod) achieved by the hardware accelerated communication. The reported results are obtained directly using the adaptive locomotion control deployed on the robot that is requested to perform free swinging of the legs without any obstacles nor ground. The estimated and real errors are shown in Fig. 9.

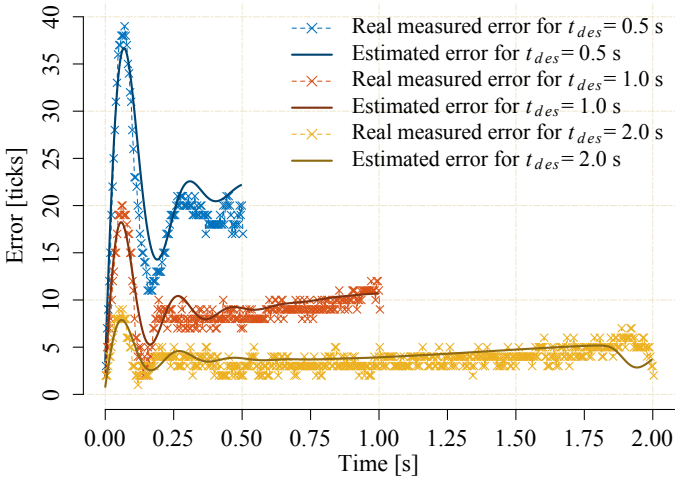

Figure 9: Estimated and real position errors for the leg motion speed defined as $t_{des} \in \{0.5, 1.0, 2.0\}$ in seconds and $t_{con} = 3$ ms.

It can be seen from the results that the estimated error value matches the real error value, which supports a high-fidelity of the developed dynamic model to adjust the value of the threshold e_{thld} for the proposed position controller. Furthermore, the error plots in Fig. 9 explain the problem with the former adaptive locomotion [14] approach that uses a fixed threshold value. The rapid increase in the error at the beginning of the swing-down phase would require a very high value of the single fixed threshold. The reliable locomotion for the former approach [14] is observed for $t_{des} \leq 1$ s, albeit shorter periods are also possible at the cost of the servomotors overheating, and thus suitable only for short deployments. Hence, the proposed approach supports scalability to both different gaits and different speeds of the motion.

8.2. Locomotion Stability using Different Motion Gaits

The reliability of the ground detection and precision of the error estimation greatly influences the stability of the robot during the locomotion. Therefore, we have experimentally verified the proposed controller in traversing rough terrains.[2] The reliability of the ground detection is measured by observing the body motion during the swing-down phase of the leg.

The locomotion stability has been evaluated using the terrain mockup shown in Fig. 10, and we quantify the body motion using readings from XSens MTi-30 AHRS attached

[2]The robot traversing the terrains is shown in the accompanying video from the real deployment at `https://youtu.be/Tdzt4yDQWI0`.

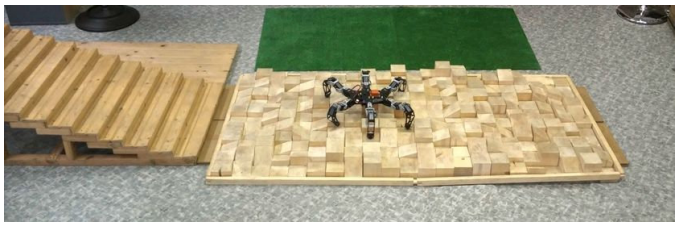

Figure 10: Used terrain mockup with three terrain types: blocks, stairs, and flat.

to the hexapod body. The used terrain mockup consists of three different terrains: wooden blocks with dimensions 10 × 10 cm and variable height and slope, wooden stairs with the step height of 4 cm, and flat ground.

We have measured the body orientation (pitch and roll angles) and the linear acceleration in the vertical direction (Acc_z) during the leg swing-down phase for three motion gaits for the former method [14] with the fixed threshold value and for the adaptive model-based adjustment of the threshold value in the proposed adaptive locomotion control.

The pitch, roll, and acceleration variables are measured with 400 Hz during the leg swing-down phase until all the active legs reach the ground. Then, variances of the variables are computed from the collected data per each leg as the performance indicators, and the five-number summary for all the indicators is visualized in Fig. 11a–Fig. 11c for the pitch, roll, and Acc_z, respectively. The value of $t_{des} = 1$ s is selected for both approaches because the used terrain mockup is relatively short and the former approach [14] exhibited sufficient robustness in the experimental verification for such a short deployment. The reported results confirm the motion stability is increased in comparison to the groundwork [14].

8.3. Cost of Transport and Locomotion Speed

Next, we consider the *Cost of Transport* (CoT) as the locomotion performance indicator together with the achieved speed of the locomotion in different terrains using the experimental mockup. We follow the CoT defined by [4] as

$$\mathrm{CoT} = P/(mgv), \tag{18}$$

where P is the instantaneous power consumption, $m = 2.3$ kg is the mass of the robot, $g = 9.81$ ms^{-2} is the gravitational constant, and v is the speed of the robot computed as the traveled distance of the robot per one second. The power consumption has been obtained from the measured voltage and current drawn directly from the battery that is measured with the sampling frequency 1 kHz. The speed has been estimated using an external visual localization system based on [49] running at 25 Hz as $v = ds/dt$, where ds is the measured robot displacement within the period $dt = 10$ s. Hence, the more frequent power data are averaged over the moving window of 10 s.

Table 4: Achieved values of the cost of transport and locomotion speed using different gaits and fixed and proposed threshold settings for the position-based ground detection

Gait	t_{des} [s]	**Ground Detection**	**CoT** [–]	**Speed** [m.s^{-1}]
Tripod	0.5	Fixed [14]	25.9	0.044
		Proposed	**22.0**	**0.046**
	1	Fixed [14]	35.4	**0.041**
		Proposed	**16.1**	0.035
Tetrapod	0.5	Fixed [14]	**29.4**	0.034
		Proposed	32.4	**0.035**
	1	Fixed [14]	19.6	0.029
		Proposed	**19.3**	**0.030**
Pentapod	0.5	Fixed [14]	28.5	0.021
		Proposed	**27.4**	**0.028**
	1	Fixed [14]	28.5	**0.019**
		Proposed	**28.4**	0.017

We consider all three motion gaits with the fixed value threshold-based approach [14] and the proposed model-based approach in this experimental evaluation. Two values of $t_{des} \in \{0.5, 1.0\}$ in seconds are considered to highlight the reduced power consumption in fast locomotion by the improved ground detection. For each parametrization, three trials have been performed, and the averaged values of the indicators are summarized in Table 4.

The results show that the proposed approach achieves lower values of the CoT in comparison to the groundwork [14] in all scenarios except the tetrapod gait and $t_{des} = 0.5$ s. As the CoT metric depends on the current readings that are proportional to the torques acting on the robot joints, we conclude that the proposed approach with dynamic thresholding achieves better performance in the ground detection, which leads to the lower stress put on the robot construction; hence, lower torques. Note, the locomotion speed is due to the same parametrization of the gaits almost similar, with the fastest being the tripod gait and the slowest the pentapod gait.

8.4. Locomotion Reliability

The proposed model-based thresholding should positively influence the stress put on the robot construction in comparison to the fixed value threshold-based approach [14]. The adaptive thresholding avoids high torque values at the foot-strike detection as can be seen in Fig. 7. Since the real torque values are not available for the utilized Dynamixel AX-12A servomotor, the real expected benefit of lower torques can be measured by a temperature that can be read out from the servomotors. Therefore, we performed an additional experiment with record-

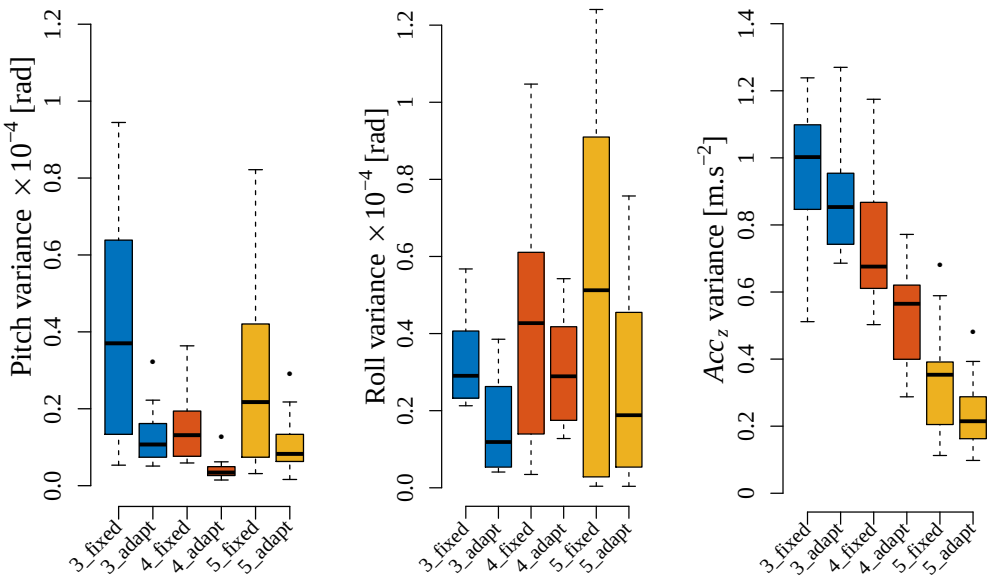

(a) Pitch Variance (b) Roll Variance (c) Acc_z Variance

Figure 11: Stability of the locomotion for different gaits and ground detection methods. The gait names at the x-axis values encode the motion gait and the used algorithm, e.g., the gait name 3_fixed correspond to the tripod gait and groundwork method [14] with the fixed valued of the threshold. The proposed ground detection with the model-based adaptive adjustment of the threshold is denoted 3_adapt. The results for the tetrapod and pentapod gait start with 4 and 5, respectively.

ing the temperature of the femur and tibia servomotors while traversing the experimental mockup. The temperature is read out after each gait cycle of the tripod gait with $t_{des} = 1\,\text{s}$. The fix value of the threshold $e_{thld} = 21$ has been utilized as the former approach [14]. Three experimental trials have been performed for the fixed e_{thld} and the proposed adaptive thresholding. There was a pause after each trial with the robot only standing in the default position on the flat ground to let the servomotors cool down to approximately 37°C, which is an average temperature of the servomotors when the robot is not moving.

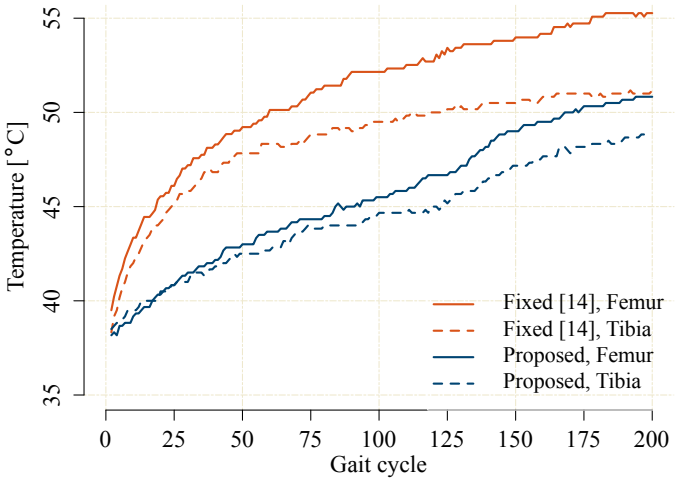

Figure 12: Evolution of the mean temperature of the femur and tibia servomotors during the robot locomotion on the experimental terrain mockup for the fixed threshold approach [14] with $e_{thld} = 21$ and the proposed adaptive model-based thresholding with $\epsilon = 3$.

The evolution of the temperature during approximately ten minutes long traversing is visualized in Fig. 12.

The temperature evolution demonstrates a positive impact of the proposed adaptive model-based thresholding on the torque values as the temperature is significantly lower than for the fixed threshold value. The room temperature was about 22°C during the experiment, and thus the servomotor limit 70°C, for which the servomotor automatically shutdowns, has not been reached. However, such a behavior has been observed for the fixed threshold and an intensive operation during summer without air conditioning in the room. The reported results support the proposed adaptive thresholding lowers the overall stress put on the robot construction and prevents the servomotor from overheating. It can also be observed that the tibia servomotor heats less than the femur servomotor which generally suggests lower torques in the femur joints. This further advocates choice of using only the femur servomotor for the ground contact detection.

9. Conclusion

In this paper, we present a minimalistic adaptive locomotion control approach for affordable hexapod walking robots that utilizes only the position feedback from the servomotors to provide a tactile sensing capability, and thus enables traversing rough terrains. The proposed locomotion consists of the two parts: the ground sensing and body leveling, which adjust the position of the robot trunk to maintain a stable position of the robot and moves it forward. The proposed ground detection is based on

monitoring of the joint position error, where the appropriate threshold value is estimated by the developed dynamic model of the leg that is accompanied by a model of the internal controller of the used servomotors.

The proposed approach has been experimentally verified using a real hexapod walking robot in traversing experimental mockup with three terrain types. The proposed locomotion control successfully traversed the terrains with three motion gaits using only the position feedback from the servomotors and provides more reliable and stable locomotion with lower power consumption than the previous approach based on a single fixed value of the position error threshold used for the ground detection and triggering the leg motion control.

The developed dynamic model can be generalized to different kinematic chains, and thus the proposed locomotion control can be applied to different multi-legged robots. The herein presented solution employs only two joints that are active during the swing-down phase that shows to be sufficient for crawling rough terrains. However, the model can be straightforwardly extended to consider more joints, and thus realize any-angle tactile sensing. Both of these generalizations are subjects of our future work.

Acknowledgment

The presented work has been supported by the Czech Science Foundation (GAČR) under research projects No. 15-09600Y and No. 18-18858S. The authors acknowledge the support of the OP VVV funded project CZ.02.1.01/0.0/0.0/16_019/0000765 "Research Center for Informatics".

[1] C.-C. Kau, K. W. Olson, E. A. Ribble, C. A. Klein, Design and implementation of a vision processing system for a walking machine, IEEE Transactions on Industrial Electronics 36 (1) (1989) 25–33. doi:10.1109/41.20341.

[2] U. Saranli, M. Buehler, D. E. Koditschek, RHex: A simple and highly mobile hexapod robot, International Journal of Robotics Research (IJRR) 20 (7) (2001) 616–631. doi:10.1177/02783640122067570.

[3] A. Elfes, R. Steindl, F. Talbot, F. Kendoul, P. Sikka, T. Lowe, N. Kottege, M. Bjelonic, R. Dungavell, T. Bandyopadhyay, others, The Multilegged Autonomous eXplorer (MAX), in: IEEE International Conference on Robotics and Automation (ICRA), 2017, pp. 1050–1057. doi:10.1109/ICRA.2017.7989126.

[4] M. Bjelonic, N. Kottege, P. Beckerle, Proprioceptive control of an over-actuated hexapod robot in unstructured terrain, in: IEEE/RSJ International Conference on Intelligent Robots and Systems (IROS), 2016, pp. 2042–2049. doi:10.1109/IROS.2016.7759321.

[5] C. Semini, V. Barasuol, T. Boaventura, M. Frigerio, M. Focchi, D. G. Caldwell, J. Buchli, Towards versatile legged robots through active impedance control, International Journal of Robotics Research (IJRR) 34 (7) (2015) 1003–1020. doi:10.1177/0278364915578839.

[6] A. Roennau, G. Heppner, M. Nowicki, R. Dillmann, LAURON V: A versatile six-legged walking robot with advanced maneuverability, in: IEEE/ASME International Conference on Advanced Intelligent Mechatronics (AIM), 2014, pp. 82–87. doi:10.1109/AIM.2014.6878051.

[7] X. Xiong, F. Wörgötter, P. Manoonpong, Neuromechanical control for hexapedal robot walking on challenging surfaces and surface classification, Robotics and Autonomous Systems 62 (12) (2014) 1777–1789. doi:10.1016/j.robot.2014.07.008.

[8] D. Belter, K. Walas, A Compact Walking Robot – Flexible Research and Development Platform, in: Recent Advances in Automation, Robotics and Measuring Techniques, Advances in Intelligent Systems and Computing, Springer, Cham, 2014, pp. 343–352. doi:10.1007/978-3-319-05353-0_33.

[9] M. Gorner, T. Wimbock, A. Baumann, M. Fuchs, T. Bahls, M. Grebenstein, C. Borst, J. Butterfass, G. Hirzinger, The DLR-Crawler: A testbed for actively compliant hexapod walking based on the fingers of DLR-Hand II, in: IEEE/RSJ International Conference on Intelligent Robots and Systems (IROS), 2008, pp. 1525–1531. doi:10.1109/IROS.2008.4650655.

[10] F. Tedeschi, G. Carbone, Design issues for hexapod walking robots, Robotics 3 (2) (2014) 181–206. doi:10.3390/robotics3020181.

[11] F. Ozguner, S. J. Tsai, Design and Implementation of a Binocular-Vision System for Locating Footholds of a Multi-Legged Walking Robot, IEEE Transactions on Industrial Electronics IE-32 (1) (1985) 26–31. doi:10.1109/TIE.1985.350137.

[12] J. G. Cham, S. A. Bailey, J. E. Clark, R. J. Full, M. R. Cutkosky, Fast and robust: Hexapedal robots via shape deposition manufacturing, International Journal of Robotics Research (IJRR) 21 (10-11) (2002) 869–882. doi:10.1177/0278364902021010837.

[13] R. Full, D. Koditschek, Templates and anchors: neuromechanical hypotheses of legged locomotion on land, Journal of Experimental Biology 202 (23) (1999) 3325–3332.

[14] J. Mrva, J. Faigl, Tactile sensing with servo drives feedback only for blind hexapod walking robot, in: 10th International Workshop on Robot Motion and Control (RoMoCo), 2015, pp. 240–245. doi:10.1109/RoMoCo.2015.7219742.

[15] R. W. Jung, ROBOTIS-GIT/DynamixelSDK, cited on 2018-08-01.
URL `https://github.com/ROBOTIS-GIT/DynamixelSDK/blob/master/c\%2B\%2B/src/dynamixel_sdk/port_handler_linux.cpp`

[16] N. Kottege, C. Parkinson, P. Moghadam, A. Elfes, S. P. Singh, Energetics-informed hexapod gait transitions across terrains, in: IEEE International Conference on Robotics and Automation (ICRA), 2015, pp. 5140–5147. doi:10.1109/ICRA.2015.7139915.

[17] M. Kalakrishnan, J. Buchli, P. Pastor, S. Schaal, Learning locomotion over rough terrain using terrain templates, in: IEEE/RSJ International Conference on Intelligent Robots and Systems (IROS), 2009, pp. 167–172. doi:10.1109/IROS.2009.5354701.

[18] D. Belter, P. Skrzypczyński, Rough terrain mapping and classification for foothold selection in a walking robot, Journal of Field Robotics 28 (4) (2011) 497–528. doi:10.1002/rob.20397.

[19] X. Shao, Y. Yang, W. Wang, Obstacle crossing with stereo vision for a quadruped robot, in: International Conference on Mechatronics and Automation (ICMA), 2012, pp. 1738–1743. doi:10.1109/ICMA.2012.6284399.

[20] D. Belter, P. Łabęcki, P. Skrzypczyński, An exploration-based approach to terrain traversability assessment for a walking robot, in: IEEE International Conference on Safety, Security, and Rescue Robotics (SSRR), 2013. doi:10.1109/SSRR.2013.6719331.

[21] D. Belter, P. Labecki, P. Skrzypczynski, Adaptive Motion Planning for Autonomous Rough Terrain Traversal with a Walking Robot: Adaptive Motion Planning for Autonomous Rough Terrain Traversal with a Walking Robot, Journal of Field Robotics 33 (3) (2016) 337–370. doi:10.1002/rob.21610.

[22] K. Walas, Improving accuracy of local maps with active haptic sensing, in: K. Kozlowski (Ed.), Robot Motion and Control 2011, Vol. 422 of Lecture Notes in Control and Information Sciences, Springer London, 2012, pp. 137–146.

[23] V. Barasuol, J. Buchli, C. Semini, M. Frigerio, E. R. De Pieri, D. G. Caldwell, A reactive controller framework for quadrupedal locomotion on challenging terrain, in: International Conference on Robotics and Automation (ICRA), 2013, pp. 2554–2561. doi:10.1109/ICRA.2013.6630926.

[24] I. Havoutis, C. Semini, J. Buchli, D. G. Caldwell, Quadrupedal trotting with active compliance, in: IEEE International Conference on Mechatronics (ICM), IEEE, 2013, pp. 610–616. doi:10.1109/ICMECH.2013.6519112.

[25] M. Focchi, V. Barasuol, I. Havoutis, J. Buchli, C. Semini, D. G. Caldwell, Local reflex generation for obstacle negotiation in quadrupedal locomotion, Nature-Inspired Mobile Robotics (2013) 443–450doi:10.1142/9789814525534_0056.

[26] J. Porta, E. Celaya, Reactive free-gait generation to follow arbitrary trajectories with a hexapod robot, Robotics and Autonomous Systems 47 (4) (2004) 187–201. doi:10.1016/j.robot.2004.04.001.

[27] A. Prochazka, D. Gillard, D. J. Bennett, Implications of positive feedback in the control of movement, Journal of Neurophysiology 77 (6) (1997) 3237–3251. doi:10.1152/jn.1997.77.6.3237.

[28] A. Winkler, I. Havoutis, S. Bazeille, J. Ortiz, M. Focchi, R. Dillmann, D. Caldwell, C. Semini, Path planning with force-based foothold adaptation and virtual model control for torque controlled quadruped robots, in: IEEE International Conference on Robotics and Automation (ICRA), 2014, pp. 6476–6482. doi:10.1109/ICRA.2014.6907815.

[29] He Zhang, Rui Wu, Changle Li, Xizhe Zang, Xuehe Zhang, Hongzhe Jin, Jie Zhao, A Force-Sensing System on Legs for Biomimetic Hexapod Robots Interacting with Unstructured Terrain, Sensors 17 (7) (2017) 1514. doi:10.3390/s17071514.

[30] K. Walas, Tactile sensing for ground classification, Journal of Automation, Mobile Robotics & Intelligent Systems 7 (2) (2013) 18–23.

[31] K. Walas, Foot design for a hexapod walking robot, Pomiary Automatyka Robotyka 17 (2013) 283–287.

[32] K. Walas, D. Belter, Messor-Verstatile wal king robot for serach and rescue missions, Journal of Automation Mobile Robotics and Intelligent Systems 5 (2011) 28–34.

[33] M. Agheli, S. S. Nestinger, Force-based stability margin for multi-legged robots, Robotics and Autonomous Systems 83 (2016) 138–149. doi:10.1016/j.robot.2016.05.012.

[34] P. Arena, P. Furia, L. Patané, M. Pollino, Fly-inspired sensory feedback in a reaction-diffusion neural system for locomotion control in a hexapod robot, in: International Joint Conference on Neural Networks (IJCNN), 2015, pp. 1–8. doi:10.1109/IJCNN.2015.7280544.

[35] M. Bjelonic, N. Kottege, T. Homberger, P. Borges, P. Beckerle, M. Chli, Weaver: Hexapod robot for autonomous navigation on unstructured terrain, Journal of Field Robotics 35 (7) (2018) 1063–1079. doi:10.1002/rob.21795.

[36] M. Travers, J. Whitman, H. Choset, Shape-based coordination in locomotion control, International Journal of Robotics Research (IJRR) 0 (0) (2018) 0278364918761569. doi:10.1177/0278364918761569.

[37] M. Palankar, A distributed local-leg feedback algorithm for robust walking on uneven terrain, Ph.D. thesis, University of South Florida (May 2013).

[38] M. Palankar, L. Palmer, A force threshold-based position controller for legged locomotion: Toward local leg feedback algorithms for robust walking on uneven terrain, Autonomous Robots 38 (3) (2015) 301–316. doi:10.1007/s10514-014-9413-0.

[39] K. Walas, D. Belter, Supporting locomotive functions of a six-legged walking robot, International Journal of Applied Mathematics and Computer Science 21 (2) (2011) 363–377.

[40] G. Best, P. Moghadam, N. Kottege, L. Kleeman, Terrain classification using a hexapod robot, in: Proceedings of the Australasian Conference on Robotics and Automation (ACRA), 2013.

[41] J. Mrva, J. Faigl, Feature extraction for terrain classification with crawling robots, in: Proceedings ITAT 2015: Information Technologies - Applications and Theory, 2015, pp. 179–185.

[42] M. Stejskal, J. Mrva, J. Faigl, Road following with blind crawling robot, in: IEEE International Conference on Robotics and Automation (ICRA), 2016, pp. 3612–3617. doi:10.1109/ICRA.2016.7487544.

[43] W. Chen, G. Ren, J. Zhang, J. Wang, Smooth transition between different gaits of a hexapod robot via a central pattern generators algorithm, Journal of Intelligent & Robotic Systems 67 (3) (2012) 255–270. doi:10.1007/s10846-012-9661-1.

[44] D. Belter, Gait modification strategy for a six-legged robot walking on rough terrain, in: 15th International Conference on Climbing and Walking Robots, Adaptive Mobile Robotics, World Scientific, 2012, pp. 367–374. doi:10.1142/9789814415958_0048.

[45] J. Paskarbeit, M. Schilling, J. Schmitz, A. Schneider, Obstacle crossing of a real, compliant robot based on local evasion movements and averaging of stance heights using singular value decomposition, in: IEEE International Conference on Robotics and Automation (ICRA), 2015, pp. 3140–3145. doi:10.1109/ICRA.2015.7139631.

[46] B. Siciliano, L. Sciavicco, L. Villani, G. Oriolo, Robotics: Modelling, Planning and Control, Springer Science & Business Media, 2010. doi:10.1007/978-1-84628-642-1.

[47] P. Čížek, J. Mrva, J. Faigl, Adaptive locomotion control, cited on 2018-09-12.
URL `http://purl.org/comrob/adaptive`

[48] J. Nishii, An analytical estimation of the energy cost for legged locomotion, Journal of theoretical biology 238 (3) (2006) 636–645. doi:10.1016/j.jtbi.2005.06.027.

[49] E. Olson, AprilTag: A Robust and Flexible Visual Fiducial System, in: IEEE International Conference on Robotics and Automation (ICRA), 2011, pp. 3400–3407. doi:10.1109/ICRA.2011.5979561.